



Non-destructive characterization of materials and components with neutron and X-ray diffraction methods

by A.M. Venter*

Synopsis

The availability of advanced characterization techniques is integral to the development of advanced materials, not only during development phases, but in the manufactured components as well. At Necsa, two modern neutron diffractometers equipped with *in-situ* sample environments, as well as complementary X-ray diffraction instruments, are now available as User Facilities within the National System of Innovation in support of the South African research and industrial communities. Neutrons and X-rays, owing to their different interaction mechanisms with matter, offer complementary techniques for probing crystalline materials. Both techniques enable nondestructive investigation of phenomena such as chemical phase composition, residual stress, and texture (preferred crystallite orientation). More specifically, the superior penetration capabilities of thermal neutrons into most materials allows for the analysis of bulk or localized depth-resolved properties in a wide variety of materials and components. Materials that can be investigated include metals, alloys, composites, ceramics, and coated systems. In particular, depth-resolved analyses using neutron diffraction complements surface investigations using laboratory X-rays in many scientific and engineering topics. The diffraction techniques can add significant downstream value to the anticipated nuclear industry development activities.

Keywords

residual stress; crystallographic texture; chemical phase identification, neutron and X-ray diffraction.

Introduction

Materials characterization is central in understanding the relationship between the structure, properties, and performance in order to engineer materials that fit the performance criteria for specific applications. This is conveniently represented in the form of a tetrahedron, generally known as the material science paradigm (Figure 1).

The availability of advanced characterization techniques is integral to the development of advanced metals, not only during development phases, but in the form of manufactured components. At Necsa (South African Nuclear Energy Corporation), modern X-ray and neutron diffraction instruments are now accessible to the South African research and industrial communities. These facilities enable nondestructive investigations of materials and components that could add significant downstream value to the anticipated nuclear industry development activities.

Background

Approximately 95% of solid materials can be described as crystalline. By applying the wave properties of X-rays (keV energies as generated in laboratory-based units, or high-power synchrotron facilities) and neutrons (meV energies) having wavelengths of the same order as atomic spacings, *i.e.* 10⁻¹⁰ m, unique information can be obtained. Their interaction with the crystalline ordering leads to constructive interference described by Bragg's law of diffraction. This leads to characteristic diffraction patterns for each phase that essentially are fingerprints of the chemical phase content (Fourier transform of the atomic arrangement). Both the peak positions (corresponding to lattice plane spacings) and the relative intensities (corresponding to the atomic species and arrangement in the unit cell) in the diffraction patterns are indicative of specific phases. X-ray photons scatter through an electromagnetic interaction with the electron charge cloud of the material, while neutrons are scattered by interaction with the nuclei. In general the interaction strength of X-rays with matter is directly related to the atomic number of the materials being investigated, whereas neutron scattering lengths are approximately equal in magnitude for most atoms. Apart from the interaction strength differences, their penetration depths are also dependent on the atomic species, as summarized in Table I for a number of technologically important materials.

The different interaction mechanisms of neutrons and X-rays with matter offer complementary techniques for investigating crystalline materials at the microstructural

* Research and Development Division, The South African Nuclear Energy Corporation SOC Ltd., (Necsa), Pretoria, South Africa.

© The Southern African Institute of Mining and Metallurgy, 2015. ISSN 2225-6253. Paper received Aug. 2015 and revised paper received Aug. 2015.

Non-destructive characterization of materials and components

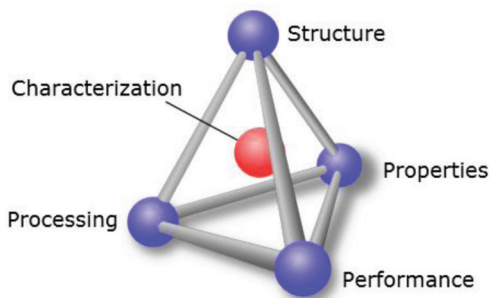


Figure 1 – Material science paradigm

level. Both techniques enable nondestructive investigation of phenomena such as chemical phase composition, residual stress, and texture (preferred crystallite orientation). Materials include metals, alloys, composites, ceramics, and coated systems. In particular, depth-resolved analysis using neutron diffraction complements surface investigations using laboratory X-rays in many scientific and engineering disciplines.

Neutrons complement X-rays due to the following properties:

- Neutrons are electrically neutral. This enables orders of magnitude deeper penetration of bulk material/components:
 - Allows nondestructive bulk analysis
 - Ease of *in situ* experiments, *e.g.* variable temperature, pressure, magnetic field, chemical reaction, *etc.*
- Neutrons detect light atoms even in the presence of heavy atoms (organic crystallography) – especially hydrogen. This property has been decisive in the investigation of high-temperature superconductors
- Neutrons distinguish atoms adjacent in the periodic table, and even isotopes of the same element (changing scattering picture without changing chemistry). This is particularly applicable to the transition metal series
- Neutrons have a magnetic moment. This enables nondestructive investigation of magnetic phenomena from direct observation of the reciprocal lattice.

Neutrons of adequate flux for neutron diffraction applications are produced as a by-product of the fission of ^{235}U in neutron research reactors (such as SAFARI-1 operated by Necsa in South Africa), or in accelerator-based facilities when very high-energy protons strike a target producing 'spallation'. These high-energy (MeV) neutron products are then thermalized and filtered to the thermal energy range (meV).

The neutron diffraction instruments at SAFARI-1 operate in constant wavelength mode where a highly monochromatic thermal neutron beam (<1% wavelength spread with wavelengths selectable in the range 1.0–2.0 Å, typically 25 meV energies) with a flux in the order of 10^6 neutrons per square centimetre per second is extracted from the fission energy spectrum and directed to a sample. Bragg's law of elastic diffraction

$$n\lambda = 2d_{hkl}\sin\theta_{hkl}$$

describes the geometrical condition for coherent diffraction that can be measured to high precision on a diffractometer. In this equation λ is the monochromatic wavelength in Å (10^{-10} m), d_{hkl} is the interatomic spacing between the parallel crystallite planes of Å dimension (hkl refers to the Miller notation of the crystal planes) and θ_{hkl} is the angle at which the diffracted peak is measured. In the angular dispersive operational mode of the SAFARI-1 neutron diffraction instruments, the wavelength is selected with the instrumental setup and thus accurately known, with d_{hkl} and θ_{hkl} being the only variables. The latter is measured experimentally to high precision with the diffraction instrument, which comprises a goniometer for sample positioning, and a detector that is precisely rotated around the goniometer axis in the horizontal plane. The diffracted intensity is measured with a high-sensitivity neutron detector that uses ^3He as ionization medium for the accurate measurement of the diffraction angles from all coherently scattered Bragg peaks from which respective values can be calculated.

As is the case with X-rays, all crystalline materials (even chemically multi-phased materials) placed in the neutron beam produces a diffraction pattern. This document provides an overview of a subset of diffraction techniques that may be of relevance to the materials beneficiation aims of the Advanced Materials Initiative.

Table I

Neutron and X-ray scattering parameters for a number of elements that comprise the common engineering alloys. Half attenuation lengths correspond to the thickness of material that reduces the intensity by 50%. 1.5 Å X-rays correspond to Cu radiation (8 keV). 0.15 Å X-rays correspond to synchrotron radiation (100 keV)

Element	Neutron coherent scattering length (b_c) [fm = 10^{-15} m]	X-ray scattering length (f_0 at $\sin\theta/\lambda = 0.2$) [fm = 10^{-15} m]	Half attenuation lengths		
			1.8 Å neutrons [mm]	1.5 Å X-rays [μm]	0.15 Å X-rays [mm]
Mg	5.375	0.246	43	100	24
Al	3.449	0.258	66	52	15
Ti	-3.37	0.451	12	11	6
Fe	9.54	0.565	20	20	2.4
Co	2.49	0.594	2	14	2
Ni	10.3	0.624	3	16	1.8
Zr	7.16	0.884	24	8	1.1
Hf	7.77	1.715	1	3	0.1
W	4.86	1.762	5	2	0.1
U	8.417	2.172	9	1	0.2

Non-destructive characterization of materials and components

Applications

Results from selected typical applications pursued at the Necsa facilities are reported to provide an indication of the potential value adding that these techniques could offer.

Chemical phase identification

The most widespread use of powder (polycrystalline) diffraction is in chemical phase analysis. This encompasses phase identification (search/match), investigation of high- and low-temperature phases, solid solutions, and determinations of unit cell parameters of new materials. A multi-phase mixture, *e.g.* a soil sample, will show more than one pattern superposed, allowing for determination of the relative concentrations of phases in the mixture.

The powder diffraction method is well suited for characterization and identification of polycrystalline phases. This is done against the International Center Diffraction Data (ICDD) database, which contains in excess of 50 000 inorganic and 25 000 organic phases. Figure 2 shows a neutron diffraction pattern of a multi-phased sintered iron powder sample that was investigated to quantify the constituent phases. The quantification was done with the Rietveld profile refinement technique (Rietveld, 1969; Taylor, 2001), in which a theoretical line profile (a combination of the crystal system and instrumental model) is matched in a least-squares refinement approach to the measured data. Such quantitative phase analysis is now routinely used in industries ranging from cement manufacture to the oil industry and can provide detection limits of 1 weight per cent (wt.%).

Residual stress

The total stress that a component experiences in practical use is the vector sum of the applied and residual stresses. The applied stresses result from the loading forces in use and can be calculated to high precision. Residual stresses, consisting of locked-in stress that remains in a material or component after the external forces that caused the stress have been removed, are mostly only approximated qualitatively. These stresses can be introduced by any mechanical, chemical, or thermal process, such as machining, plating, and welding. Stress analysis by diffraction techniques is based on accurate measurement of lattice strain distributions (variations in interatomic spacing). Using Hooke's law, stresses are

calculated from the strain distributions. Residual stresses are a double-edged sword in material science applications. Compressive residual stresses are beneficial in applications where fatigue performance is required, being able to mitigate crack initiation and propagation. Tensile residual stresses are generally considered to be detrimental as they can lead to crack initiation and propagation. Specifically, residual stress tailoring can render substantial improvements in the optimization of component design.

X-ray and neutron radiation enable nondestructive probing at different penetration depths (Hutchings *et al.*, 2005; Fitzpatrick and Lodini, 2003; Reimers *et al.*, 2008; Webster, 2000; Ohms *et al.*, 2008; Engler and Randle, 2010) (Table I). The stress tensors are obtained from the measured strain tensors and application of Hooke's law of elasticity

$$\sigma_{ij} = \frac{1}{1/2S_2} \left[\varepsilon_{ij} - \delta_{ij} \frac{S_1}{1/2S_2 + 3S_1} \varepsilon_{ii} \right]$$

where S_1 and $1/2S_2$ are the diffraction elastic constants.

Examples from recent investigations performed using neutrons are presented to illustrate potential applications.

Welded mild steel plate

As part of an investigation into the influence of differential hardness between the weld metal and base metal on residual stress and susceptibility to stress corrosion cracking, a comprehensive two-dimensional (2D) mapping of the residual stress field, through the 17 mm plate thickness and across the weld was completed. Figure 3a indicates the 2D map of the longitudinal stress component, which is maximally influenced due to the differential longitudinal contraction. Values can be as large as the yield stress of the material. Figure 3b indicates the 2D map of this stress component after the sample had undergone a post-weld heat treatment. This treatment has been very successful in having completely relaxed the tensile stress values. Such analyses are only possible owing to the penetrating capabilities of thermal neutrons and the nondestructive nature of the measurement technique.

Laser shock-peened aluminium plate

Laser shock-peen (LSP) is an emerging cold work process used to induce compressive residual stresses in metallic

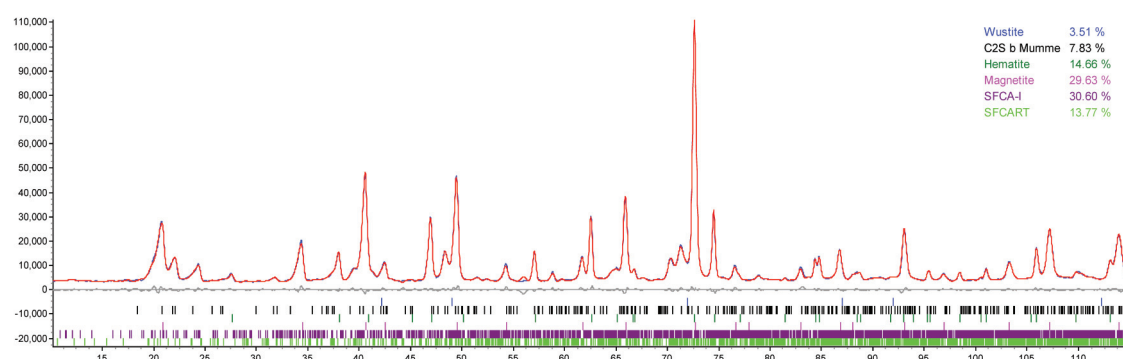


Figure 2 – Neutron powder diffraction results (measured diffracted intensities as function of diffraction angle) of a mixed-phase sintered iron sample, shown as dots (underneath the red solid line at positive intensities). The multiphase quantification results from a Rietveld analytical approach (red solid line at positive intensities) are indicated in the legend. The curve along the zero intensity level depicts the difference between the measured and analysed data and gives the goodness-of-fit. Vertical lines at negative intensities represent the Bragg peaks (hkl) corresponding to each phase

Non-destructive characterization of materials and components

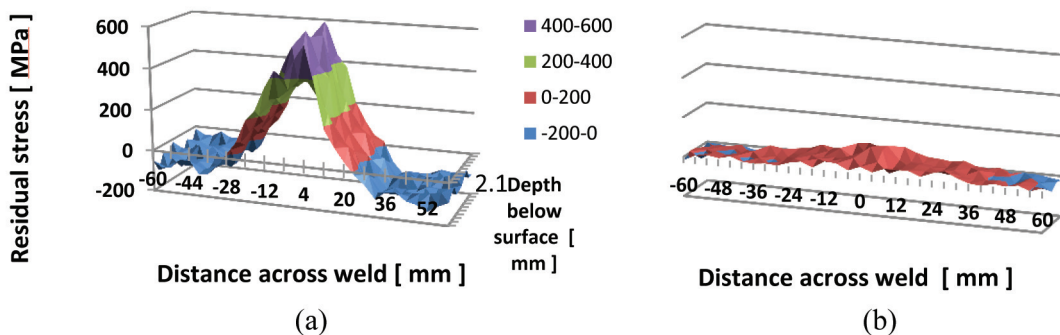


Figure 3 – Two-dimensional maps of the longitudinal residual stress component in SA 516 Gr 70 pressure vessel steel welded plates: (a) as-welded condition, (b) post-weld heat-treated condition. The weld centre-line is at 0 mm

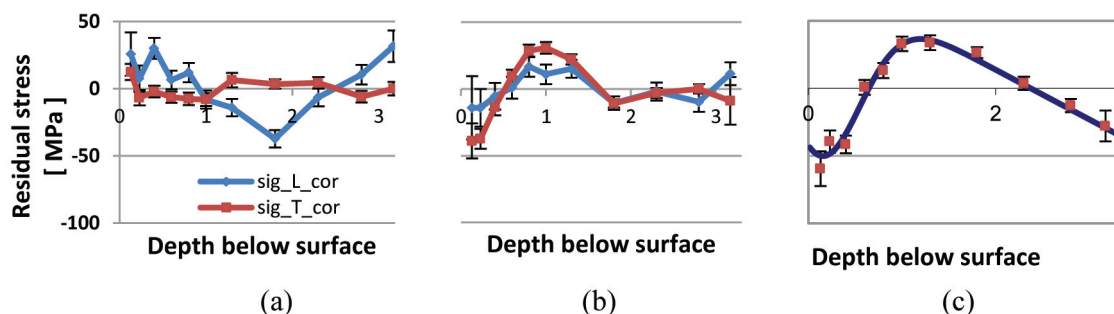


Figure 4 – Through-thickness stress profile in aluminium plate: (a) parent material, (b) laser shock-peened plate, (c) net contribution by laser shock-peen

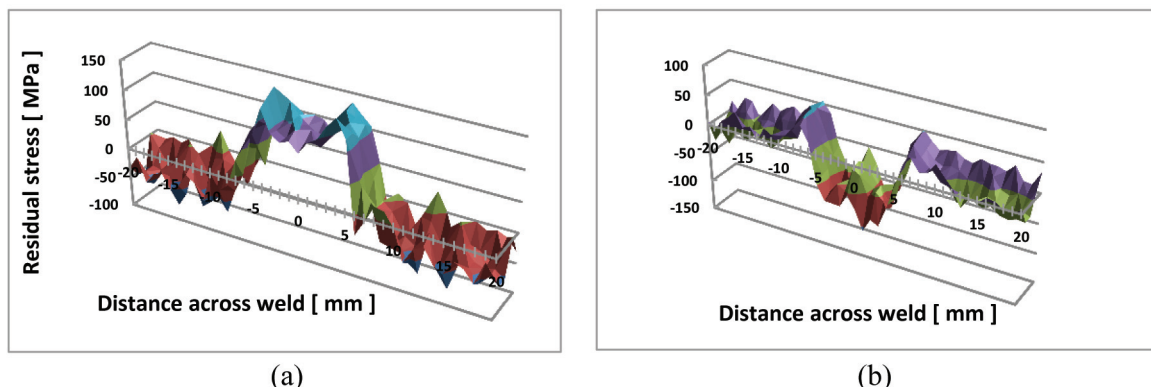


Figure 5 – 2D map of the longitudinal residual stress component in aluminium laser beam welded plates: (a) as-welded condition, (b) post-weld-treated condition after laser shock-peen treatment. The weld centre-line is at 0 mm

components to depths up to 1 mm. The purpose of this treatment is to reduce or remove tensile stresses in the surface region to improve the fatigue performance. Figure 4 summarizes the through-thickness in-plane residual stress distribution in an as-rolled aluminium AA6056-T4 plate, taken as the reference, and the stress distribution after laser shock-peen using a 3 GW laser beam. The net effect, purely due to the peen action, was determined by subtracting the reference values.

Laser-welded aluminium with laser shock peen treatment

Laser beam welding is a newly established joining technology using no filler material. Similar to other welding techniques,

it introduces adverse tensile residual stresses as well as component distortions. Figure 5 indicates 2D maps of the residual stress field measured through a 3.3 mm thick AA6056-T4 aluminium plate and across the weld.

Here again, the longitudinal stress component is most dominant, as shown in Figure 5a. To improve this adverse stress condition, the weld region has been subjected to laser shock-peen treatment using a 3 GW laser pulse. Compared to the post-weld heat treatment results given previously, the laser treatment has completely altered the tensile stress so as to be substantially compressive.

Additive-manufactured Ti-6Al-4V

In the selective laser beam melt (SLM) additive manufac-

Non-destructive characterization of materials and components

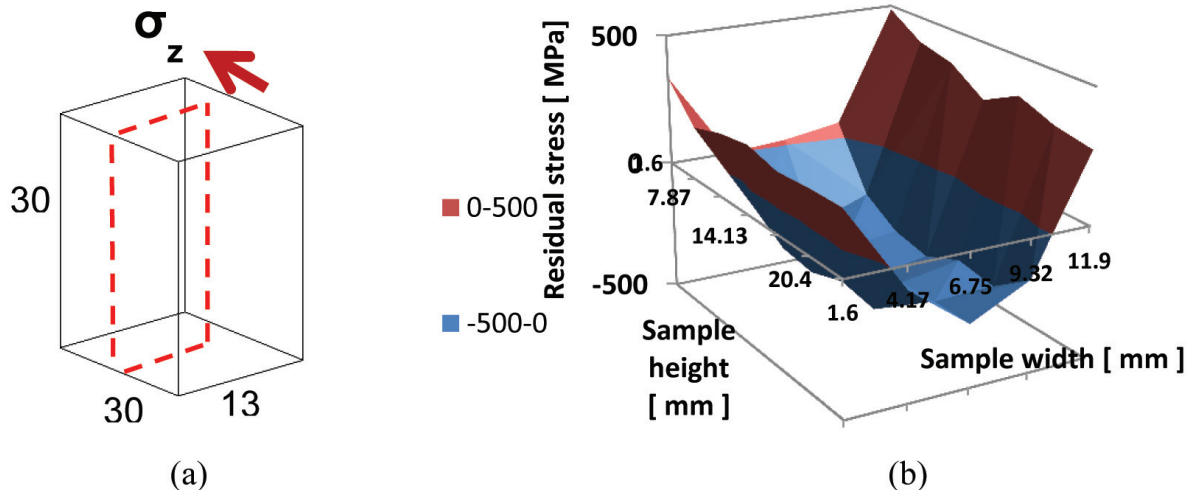


Figure 6 – Measured 2D stress component mapped perpendicular to the build direction in a SLM produced Ti-6Al-4V sample: (a) sample geometry showing the ‘internal plane’ investigated nondestructively, (b) 2D residual stress map

turing process, a high-power laser beam is used to melt and deposit successive layers of powder to form complex three-dimensional metal parts. The highly localized heat input leads to large thermal gradients. This in turn produces complex residual stress states inside the part. Figure 6 shows a stress map measured in the centre of the sample perpendicular to the build direction in a Ti-6Al-4V sample. This reveals the existence of tensile residual stresses in the near-surface regions, while the central region of the sample is in compression.

Texture analysis

Most solid-state matter has a polycrystalline structure composed of a multitude of individual crystallites or grains. The crystallographic orientation can have various arrangements, ranging from completely random to the development of preferred alignment. The significance of this texture lies in the corresponding anisotropy of many material properties. The influence could be as much as 20–50% of the property value. X-ray and neutron diffraction analysis methods are well established, rendering results referred to as

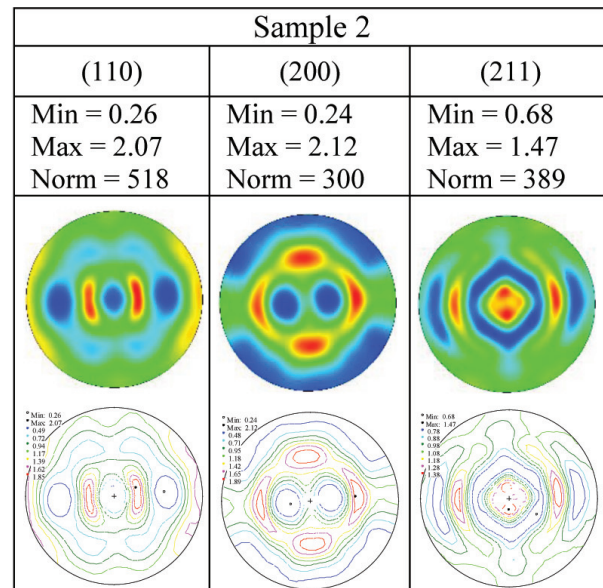
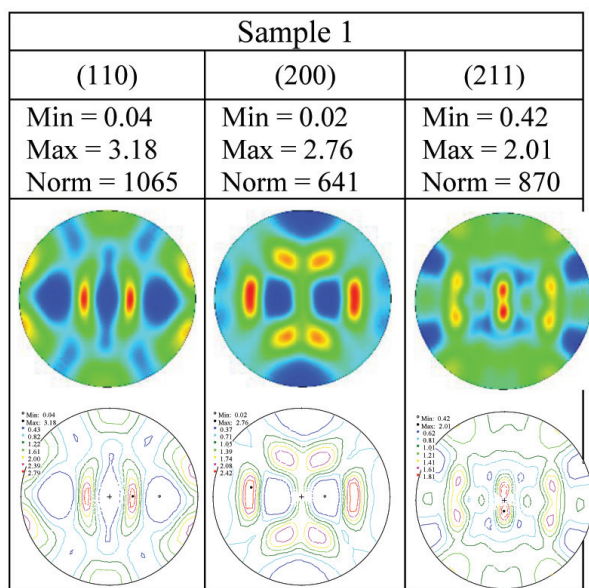


Figure 7 – Pole figure representations of selected reflections from two ferritic stainless steel samples subjected to different heat treatments, measured with neutron diffraction

Non-destructive characterization of materials and components

macro or bulk texture (Engler and Randle, 2010). Analyses can also be supplemented by methods whereby individual orientations are measured by transmission or scanning electron microscopy and are directly related to the microstructure, which has given rise to the term 'microtexture'.

The preferred orientation is usually described in terms of pole figures. The inverse pole figure gives the probability of finding a given specimen direction parallel to crystal (unit cell) directions. By collecting data for several reflections and combining several pole figures, the complete orientation distribution function (ODF) of the crystallites within a single polycrystalline phase that makes up the material can be determined (Engler and Randle, 2010).

Shown in Figure 7 are bulk pole figures measured with neutron diffraction on ferritic stainless steel specimens that have been subjected to different heat-treatment parameters after rolling. Significant texture development is evident, which will contribute to anisotropic properties that could lead to physical phenomena such as earing, warping, and general dimensional changes and distortions.

Conclusions

These examples serve to demonstrate the capabilities of the X-ray and neutron diffraction techniques available at Necsa for the characterization of new materials and advanced beneficiation techniques to enhance component performance in various applications. The vast field of applications can be reviewed in the extensive literature references provided, as well as recent publications from Necsa (Taran *et al.*, 2014; Troiano *et al.*, 2012; Venter, Luzin, and Hattingh, 2014; Venter *et al.*, 2008, 2013, 2014a, 2014b; Zhang *et al.*, 2008). Due to the nondestructive nature of the techniques, samples can be investigated at various stages of their manufacture or utilization lifetimes.

Acknowledgments

Specific acknowledgment is attributed to the various co-workers from Necsa and academia and their willingness that the results may be used in this document: Professor Johan de Villiers (University of Pretoria), Deon de Beer (University of Pretoria), Victoria Cain (University of Cape Town), Daniel Glaser (University of the Witwatersrand), and Deon Marais from Necsa.

References

ENGLER, O. and RANDLE, V. (eds). 2010. *Introduction to Texture Analysis, Macrotecture, Microtexture, and Orientation Mapping*. CRC Press, Taylor and Francis.

FITZPATRICK, M.E. and LODINI, A. 2003. *Analysis of Residual Stress by Diffraction using Neutron and Synchrotron Radiation*. Taylor and Francis.

HUTCHINGS, M.T., WITHERS, P.J., HOLDEN, T.M., and LORENTZEN, T. (eds). 2005. *Introduction to the Characterization of Residual Stress by Neutron Diffraction*. Taylor and Francis.

OHMS, C., MARTINS, R.V., UCA, O., YOUTSOS, A.G., BOUCHARD, P.J., SMITH, M., KEAVY, M., BATE, S.K., GILLES, P., WIMPORY, R.C., and EDWARDS, L. 2008. *Proceedings of 2008 ASME Pressure Vessels and Piping Conference (PVP 2008)*, Chicago, Illinois, 27–31 July 2008. (PVP2008-61913).

REIMERS, W., PYZALLA, A.R., SCHREYER, A., and CLEMENS, H. (eds). 2008. *Neutrons and Synchrotron Radiation in Engineering Materials Science*. Wiley-Vch Verlag GmbH.

RIETVELD, H.M. 1969. A profile refinement method for nuclear and magnetic structures. *Journal of Applied Crystallography*, vol. 2, no. 2. pp. 65–71. doi:10.1107/S0021889869006558

TARAN, Y., BALAGUROV, A., SABIROV, B., DAVYDOV, V., and VENTER, A. 2014. Neutron diffraction investigation of residual stresses induced in niobium-steel bilayer pipe manufactured by explosive welding. *Materials Science Forum*, vol. 768–769. pp. 697–704. doi:10.4028/www.scientific.net/MSF.768–769.697

TAYLOR, J.C. 2001. *Rietveld made easy: a practical guide to the understanding of the method and successful phase quantifications*. Sietronics Pty. Ltd., Canberra.

TROIANO, E., UNDERWOOD, J.H., VENTER, A.M., IZZO, J.H., and NORRAY, J.M. 2012. Finite element model to predict the reverse loading behavior of autofrettaged A723 and Hb7 cylinders, *Journal of Pressure Vessels and Piping*, PVT-11-1204, 041012-1.

VENTER, A.M., LUZIN V., and HATTINGH, D.G. 2014. Residual stresses associated with the production of coiled automotive springs. *Material Science Forum*, vol. 777. pp. 78–83. doi:10.4028/www.scientific.net/MSF.777.78

VENTER, A.M., OLADIJO, O.P., CORNISH, L.A., and SACKS, N. 2014a. Characterisation of the residual stresses in HVOF WC-Co coatings and Substrates. *Material Science Forum*, vol. 768–769. pp. 280–285. doi:10.4028/www.scientific.net/MSF.768–769.280

VENTER, A.M., LUZIN, V., OLADIJO, O.P., CORNISH, L.A., and SACKS, N. 2014b. Study of interactive stresses in thin WC-Co coating of thick mild steel substrate using high-precision neutron diffraction. *Materials Science Forum*, vol. 772. pp. 161–165. doi:10.4028/www.scientific.net/MSF.772.161

VENTER, A.M., OLADIJO, O.P., LUZIN, V., CORNISH, L.A., and SACKS, N. 2013. Performance characterization of metallic substrates coated by HVOF WC-Co. *Thin Solid Films*, vol. 549. pp. 330–339.

VENTER, A.M., VAN DER WATT, M.W., WIMPORY, R.C., SCHNEIDER, R., MCGRATH, P.J., and TOPIC, M. 2008. Neutron strain investigations of laser bent samples. *Materials Science Forum*, vol. 571–572. pp. 63–68.

WEBSTER, G.A. (ed.). 2000. *Neutron Diffraction Measurements of Residual Stress in a Shrink-fit Ring and Plug*. *VAMAS Report No. 38*.

ZHANG, S.Y., VENTER, A.M., VORSTER, W.J.J., and KORSUNSKY, A.M. 2008. High energy synchrotron X-ray analysis of residual plastic strains induced in shot peened steel plates. *Journal of Strain Analysis*, vol. 43, no. 4. pp. 229–241. ♦